

## Implementation of a constant fraction algorithm for improved time resolution of metallic magnetic calorimeter measurements

---

**Philip Pfäfflein,<sup>a,b,c,\*</sup> Christoph Hahn,<sup>a,b</sup> Marc Oliver Herdrich,<sup>a,c</sup>  
Felix Martin Kröger,<sup>a,c</sup> Günter Weber<sup>a,b</sup> and Thomas Stöhlker<sup>a,b,c</sup>**

<sup>a</sup>*Helmholtz Institute Jena,*

*Fröbelstieg 3, 07743 Jena, Germany*

<sup>b</sup>*GSI Helmholtzzentrum für Schwerionenforschung,*

*Planckstraße 1, 64291 Darmstadt, Germany*

<sup>c</sup>*Institute for Optics and Quantum Electronics, Friedrich Schiller University,*

*Max-Wien-Platz 1, 07743 Jena, Germany*

*E-mail: [p.pfaefflein@hi-jena.gsi.de](mailto:p.pfaefflein@hi-jena.gsi.de)*

Atomic physics of highly charged ions can be studied by high precision x-ray spectroscopy. Collision experiments at storage ring facilities are one of the most promising approaches for this, particularly when the unique capabilities of metallic magnetic calorimeters (MMC) are exploited. To obtain clear spectra from these devices, accurate time of flight measurements are crucial for background reduction. Previously a so called  $k\sigma$  trigger – which is a leading edge trigger with an adaptive threshold – has been used. In this contribution we present a further background reduction by a factor of three by applying the constant fraction discrimination (CFD) trigger in the MMC data evaluation.

*FAIR next generation scientists - 7th Edition Workshop (FAIRness2022)*

*23–27 May 2022*

*Paralia (Pieria, Greece)*

---

\*Speaker

## 1. Introduction

Precision x-ray spectroscopy of heavy, few electron ions in collisions with matter is an indispensable tool for investigations of relativistic interaction dynamics as well as for probing our understanding of the atomic structure at highest electromagnetic fields. Here, a good signal to noise ratio (SNR) is key to most precision measurements. This can either be achieved by tuning the experimental conditions in favour of the process of interest, by suppression of radiation not associated with it, or – usually – a combination of both. A well established method for background suppression is the so-called coincidence technique where one measures the arrival times of various reaction products of the process of interest and sets temporal constraints on them.

In this work we focus on collision experiments at ion storage rings, such as ESR and CRYRING@ESR of GSI, Darmstadt. In these machines the stored ions can interact with gas targets as well as free-electron targets. To be more specific, the experimental data used in this work has been obtained at the electron cooler of CRYRING@ESR [1]. It acts as a free-electron target where electrons and stored ions are interacting at close to zero collision velocity. During these collisions free electrons can recombine with projectile ions under emission of photons, a process which is termed radiative recombination (RR). If electrons are captured into an excited state of the projectile, the resulting atomic state can decay to the ground state via further photon emission, see [2] for details. The RR process therefore results in two types of particles of interest, namely photons and downcharged ions. The photon emission can be recorded by x-ray spectrometers, in case of the here presented study a metallic magnetic calorimeter (MMC) tailored for photon energies between 10 keV and 100 keV [3]. The downcharged ions are separated from the primary beam in a dipole magnet downstream from the interaction area and can be detected by a particle counter. The time of flight (TOF) from the interaction point to the corresponding detector is determined by the distance between them and the particles speed. In case of the ion its speed is determined by the beam energy. Therefore an evaluation of the temporal difference of their respective arrival times can be done. By setting a coincidence condition -meaning the difference of the arrival times of the two events needs to be within certain bounds- one can achieve an effective background reduction. In these measurements this is a suppression of photons not associated with an electron being captured into a projectile ion. Note that due to the extended reaction volume within the electron cooler as well as delayed photon emission from excited states a coincidence window of approximately 100 ns is expected as demonstrated in [2].

When using semiconductor detectors, which enable time resolutions on the level of a few tens of ns, setting coincidence conditions for background suppression is a well established method. However, for an MMC detector a similar utilisation of timing information was demonstrated for the first time only in a recent beam time at CRYRING@ESR as described in [3]. For this type of detector, the time of flight information is generated in post processing of the digitised detector signals. In previous measurement campaigns with the MMC which did not rely on precise timing information, an adaptive leading edge algorithm, also referred to as  $k\sigma$  trigger [4, 5, and references therein], has been used to determine the time of arrival of the photons. This implementation was chosen as it is reliably capable of identifying individual events in multi-hit signal traces. However, the obtained timing information exhibited a significant jitter and turned out to be not sufficient for meaningful coincidence measurements. Here we present an improved timing resolution by use of

a software implementation of the constant fraction discrimination (CFD). Both timing algorithms will be explained and their timing capabilities will be compared in this report.

## 2. Comparison of the trigger logic

As trigger we refer to any logic that is capable of identifying an event like a pulse in a signal trace and returning its timing information, i.e. the arrival time. An event can be indicated by a simple heuristic criterion like the surpassing of a threshold. More sophisticated methods of identification are for example the here described  $k\sigma$  or CFD triggers. These triggers are applied to the recorded voltage signal  $S(t)$  of the detector output channels. As the signal is digitised with a fixed sampling frequency  $f_s$ , the time for the  $i$ -th signal value  $s_i$  can be expressed as  $t_i = i \times 1/f_s$ .

### 2.1 Adaptive leading edge or $k\sigma$ trigger

The so-called  $k\sigma$  trigger is effectively a leading edge trigger with a threshold which adapts to the noise level. It works by comparing the distance of the current value  $s_i$  from the moving average  $\langle S \rangle (t_i)$  to the moving standard deviation  $\sigma_S(t_i)$  of the past signal trace. If the distance is greater than a predefined factor  $k$  times the standard deviation, the algorithm registers an event. The moving statistics functions have been implemented using the exponential moving average (EMA) (see equations 2 and 3) to account for a possible baseline drift. The EMA exponentially suppresses the influence of signal points further in the past. It therefore theoretically is an infinite impulse response filter. However, due to limited numerical precision only a finite number of samples contributes. The filter can be described by its recursive definition [6]:

$$\begin{aligned} EMA(S, t_i) &= \alpha \times s_i + (1 - \alpha) \times EMA(S, t_{i-1}) \\ EMA(S, t_0) &= s_0 \end{aligned} \quad (1)$$

Here  $0 < \alpha < 1$  is the so called smoothing factor which determines how fast past events loose influence. The moving statistics functions can therefore be expressed as:

$$\langle S \rangle (t_i) = EMA(S, t_i) \quad (2)$$

$$\sigma_S(t_i) = \sqrt{EMA(S^2, t_i) - EMA^2(S, t_i)} \quad (3)$$

The implemented trigger logic includes an inhibit, which excludes a given amount of values after the determined trigger time from the EMA for a reduction of the influence of the pulse on the EMA. The  $k\sigma$  logic is applied to the discrete derivative of the averaged signal as described by the following filter equation[4]:

$$BOX(S, t_i) = \sum_{k=i-2w_B+1}^{i-w_B} S(t_k) - \sum_{k=i-w_B+1}^i S(t_k) \quad (4)$$

The filter width  $w_B$  is chosen to match the signal rise time to suppress noise spikes in the signal. The combination of both filters allows for a better multi-hit determination compared to triggering on the raw detector signal. Due to the use of a dynamic but absolute threshold the event time determined by the trigger depends on the pulse height, i.e. assuming a fixed rise time strong pulses

will surpass the threshold faster than weaker pulses. For the use in a pulse shape analysis based on the moving window deconvolution as described in [7] this is sufficient. However this dependence leads to inferior timing performance when compared to the more sophisticated timing algorithm discussed in the next section. Nonetheless the  $k\sigma$  trigger stays a crucial part in the data processing for identifying single hit events the timing of which is then analysed by the CFD trigger.

## 2.2 Constant fraction discriminator algorithm

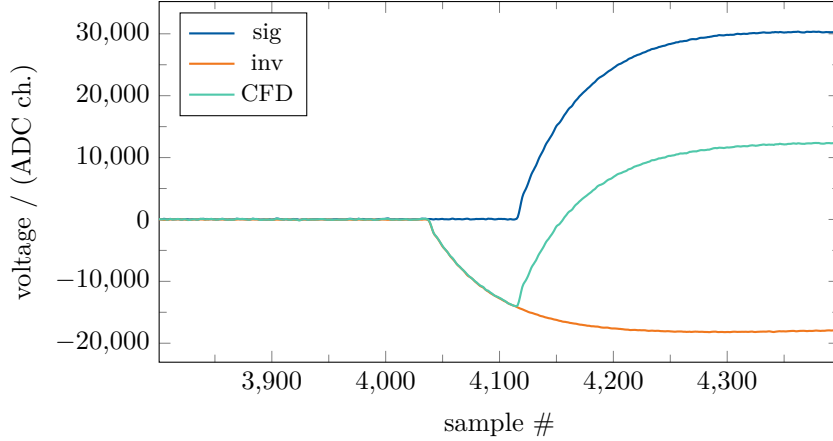


**Figure 1:** Visualisation of the signal generation for the CFD trigger algorithm: In our implementation, the input signal (blue, labeled sig) is delayed compared to the inverted and scaled signal (yellow, labeled inv). The prominent zero crossing of the sum of the two signals (green, labeled CFD) determines arrival time.

By comparison to the  $k\sigma$  trigger the CFD does not rely on absolute trigger thresholds. It rather derives the timing information at a fixed point relative to the signal height. This is achieved by superimposing the original signal with a delayed (by  $t_w$ ), scaled (by  $\lambda > 0$ ) and inverted copy of the same signal:

$$CFD(t_i) = S(t_i) - \lambda S(t_i - t_w) \quad (5)$$

One receives an output trace which has a zero crossing at a constant fraction of the initial pulse height, hence the name of this timing filter algorithm. This method is illustrated in figure 1. As the digitised signal only consists of values at discrete time steps, we perform a linear regression of points surrounding the zero crossing in order to determine the exact event timing.

## 3. Comparison of filter results

To demonstrate the timing capabilities of the new trigger engine, data recorded during the aforementioned recent experiment performed at CRYRING@ESR (see [3] for details) has been reanalysed. Figure 2 shows the TOF between the arrival of the photon and the downcharged particle plotted against the associated photon energies. The subplots compare the result of both described trigger engines. Due to the arbitrary definition of the trigger point within the signal, the absolute time of flight differs between both approaches. One can clearly see that the TOF resulting from the application of the  $k\sigma$  trigger especially for low energies results in a broader

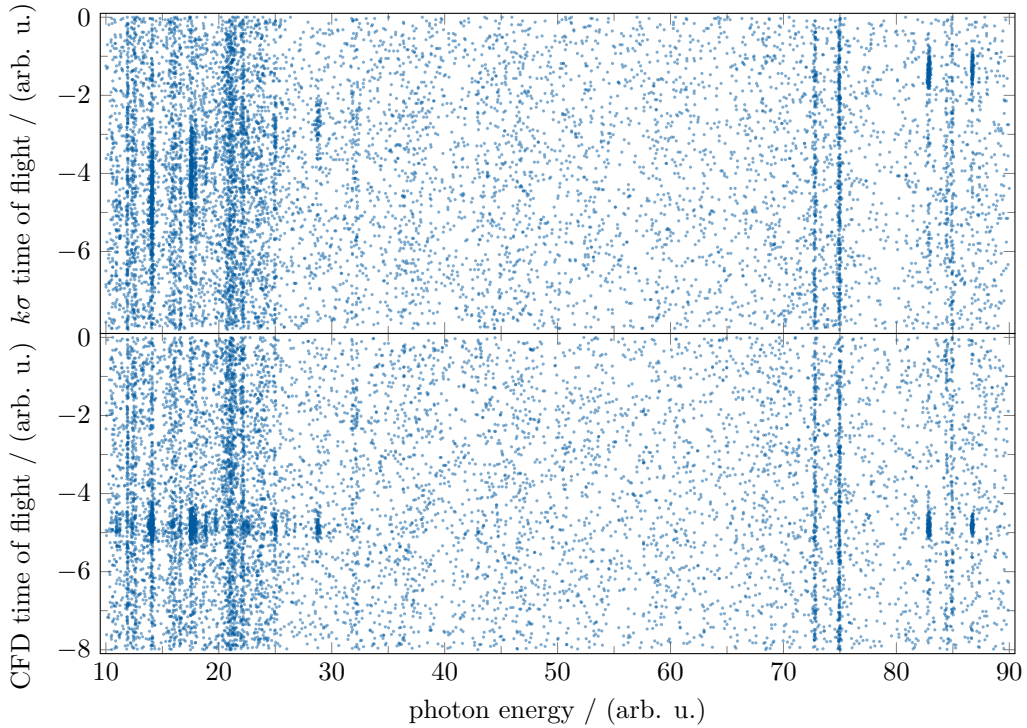


**Figure 2:** Presented are the time of flight spectra for the  $k\sigma$  trigger in the upper plot and the CFD trigger in the lower plot. Noteworthy differences are the a much broader range of arrival times for the  $k\sigma$  trigger as well as a shift in the mean arrival time with increased energy. This results in the necessity of setting a much broader coincidence window and hence including much more background into the coincident spectrum.

distribution when compared to the CFD approach. As expected, the average TOF of the individual line distributions also shows a strong dependence on the photon energy in case of the  $k\sigma$  trigger. Contrary the application of an additional CFD trigger leads to a constant timing throughout the entire spectrum. Both improvements allow for setting a narrower coincidence condition (900 ns window width for CFD compared to 7500 ns for the  $k\sigma$  trigger), thus substantially improving the background suppression.

A more detailed analysis of the resulting timing performance, also in regard of the varying signal-to-noise ratio for different pulse heights, is presented in [8]. Note that the timing filter algorithms presented in this work are not optimised for a specific detector pulse shape. In the future, it might be possible to further improve the timing resolution by using filter algorithms that contain information of the exact shape of the detector pulses.

## Acknowledgements

We would like to thank Steffen Allgeier, Andreas Fleischmann, Marvin Friedrich, Daniel Hengstler, Patricia Kuntz and Christian Enss for providing and operation of the MMC detectors. Furthermore we are grateful to Sonja Bernitt, Anton Kalinin, Michael Lestinsky, Bastian Löher, Esther Babette Menz, Tobias Over, Uwe Spillmann and Binghui Zhu for their support during the recent beamtime.

## References

- [1] Lestinsky et al., *Physics book: CRYRING@ESR*, *Eur. Phys. J. Spec. Top.* **225** (2016) 797–882.
- [2] B. Zhu et al., *X-ray emission associated with radiative recombination for  $Pb^{82+}$  ions at threshold energies*, *Phys. Rev. A* **105** (2022) 052804.
- [3] Ph. Pfäfflein et al., *Integration of maXs-type microcalorimeter detectors for high-resolution x-ray spectroscopy into the experimental environment at the CRYRING@ESR electron cooler*, *Phys. Scr.* **97** (2022) 114005.
- [4] V. I. Stoica, *Digital Pulse-Shape Analysis and Controls for Advanced Detector Systems Dissertation* Rijksuniversiteit Groningen (2012).
- [5] M. O. Herdrich, *Anwendung kryogener Kalorimeter für hoch aufgelöste Präzisions-Röntgenspektroskopie* (to be published).
- [6] R. G. Brown, *Smoothing, Forecasting and Prediction of Discrete Time Serie*, Prentice-Hall, Englewood Cliffs, N.J. 1963.
- [7] A. Georgiev et al., *An analog-to-digital conversion based on a moving window deconvolution*, *Nucl. Sci.* **41** (1994) 1116 – 1124.
- [8] Ph. Pfäfflein et al., *Exploitation of the Timing Capabilities of Metallic Magnetic Calorimeters for a Coincidence Measurement Scheme*, *Atoms* **2023** (2022) 11 (1), 5.